Impurity-induced antiferromagnetic domains in the periodic Anderson model

A. Benali,[1,2,*] Z. J. Bai,[3,†] N. J. Curro,[2,‡] and R. T. Scalettar[2,§]

[1]*Department of Physics, Faculty of Sciences of Tunis, University of Tunis El-Manar, Tunis 2092, Tunisia*

[2]*Department of Physics, One Shields Avenue, University of California, Davis, California 95616, USA*

[3]*Department of Computer Science, One Shields Avenue, University of California, Davis, California 95616, USA*

A central feature of the periodic Anderson model is the competition between antiferromagnetism, mediated by the Ruderman-Kittel-Kasuya-Yosida interaction at small conduction electron-local electron hybridization V, and singlet formation at large V. At zero temperature, and in dimension $d > 1$, these two phases are separated by a quantum critical point V_c. We use quantum Monte Carlo (QMC) simulations to explore the effect of impurities which have a local hybridization $V_* < V_c$ in the antiferromagnetic regime which are embedded in a bulk singlet phase with $V > V_c$. We measure the suppression of singlet correlations and the antiferromagnetic correlations which form around the impurity, as well as the size of the resulting domain. Exact diagonalization calculations for linear chains allow us to verify that the qualitative features obtained at intermediate coupling and finite T persist to strong coupling and $T = 0$, regimes which are difficult to access with QMC. Our calculations agree qualitatively with NMR measurements in CeCoIn$_{5-x}$Cd$_x$.

I. INTRODUCTION

The interplay of disorder and interactions results in intriguing metal-insulator, superconductor-insulator, and magnetic order-disorder transitions [1–7]. A particularly rich set of questions arises when randomness is introduced to a system which is already close to a critical point, for example through tuning the electron density or interaction strength. Here the effects of impurities might be expected to be especially large, since the system is already poised on the brink of two distinct phases.

One example of this situation is provided by the replacement of Cu by nonmagnetic atoms in cuprate superconductors where neutron-scattering studies of Zn-doped La$_{2-x}$Sr$_x$CuO$_4$ reveal the emergence of magnetic scattering peaks and the emergence of a static spin state within the spin gap [8]. Insight into this phenomenon was provided by Hartree-Fock calculations on the single band Hubbard Hamiltonian which examined the effect of local chemical potential shifts on the striped phase of coexisting d-wave superconductivity and antiferromagnetic (AF) order [9]. Local AF order was found to nucleate about the impurities above a critical threshold for the on-site interaction U. This local phase transition occurs at a different U_c for each impurity. Further theoretical work investigating the nature of local defects in quantum critical metallic systems indicates that large droplets are formed with a suppression of quantum tunneling [10]. A remarkable feature of both theory and experiment is the large extent of AF order induced by small impurity concentration. The cuprate problem is made even more complex by the large degree of inhomogeneity, e.g., in the superconducting gap, charge, and magnetic stripes, etc., that are present even without Zn doping [11,12].

Recent experiments on the replacement of In by Cd in CeCoIn$_5$ examine closely related phenomena in heavy fermions materials [13]. In this case, the parent compound CeCoIn$_5$ is already a quantum critical superconductor without the necessity of resorting to pressure or chemical doping, as is the case for La$_{2-x}$Sr$_x$CuO$_4$. In doped CeCoIn$_5$, it was found that AF islands develop about the Cd impurities, and ultimately coalesce into a magnetically ordered, but very heterogeneous, phase [14]. The inhomogeneous response of the electronic system clearly demonstrates that doping does not necessitate a quantum critical response, as observed in other heavy fermion systems [15,16]. Related issues concerning anomalous non-Fermi-liquid phases which intervene the Kondo singlet to AF transition in doped f electron alloys have also been explored [17,18].

In analogy with numerical work on the single band Hubbard Hamiltonian appropriate to modeling the cuprates, it is natural to consider a two band periodic Anderson model (PAM) [19] to understand these heavy fermion experiments [9]. One of the basic features of the PAM (when there is one electron per site) is the competition between an AF phase when the hybridization V of the conduction and localized electrons is small, and a singlet phase when V is large. Since there is no direct coupling between the local moments, their ordering arises through the Ruderman-Kittel-Kasuya-Yosida (RKKY) mechanism [20–22] in which polarization of the spin of the conduction electrons mediates an indirect interaction. In the absence of randomness, quantum Monte Carlo (QMC) has quantified this AF-singlet transition, both in the itinerant electron PAM [23] and also in quantum spin Hamiltonians which are the strong-coupling limits of the PAM, like the bilayer Heisenberg model where the interlayer exchange $J_\perp$ is varied [24,25]. The position of the quantum critical point (QCP) in the uniform system is also known in the case when one of the layers has no intralayer exchange, a geometry which is similar to that of the PAM where the f electrons are localized and have $t_{\mathrm{ff}} = 0$ [25].

Numerical work on randomness in the AF-singlet transition has thus far focused mainly on the strong-coupling, Heisenberg

*ali.benali@fst.rnu.tn

†bai@cs.ucdavis.edu

‡curro@physics.ucdavis.edu

§scalettar@physics.ucdavis.edu

spin limit. For example, Sandvik has studied how the removal of pairs of sites in a Heisenberg bilayer affects the AF-singlet quantum critical point (QCP) in the uniform system [26]. In addition to the effect of impurities on the AF-singlet transition in spin models, much is known concerning the simpler problem of the effect of a single impurity in an AF, both from numerical and field-theoretical work [27]. A focus of much of this past work has been on the behavior of the uniform susceptibility at the impurity site, where a leading order $\chi_{\rm imp} \sim 1/T$ Curie divergence is predicted, as well as a subleading logarithmic divergence. A careful QMC study of different types of impurities yields considerable insight into the origins of the various contributions to $\chi_{\rm imp}$ [27].

The distortion of the AF "spin texture" in the neighborhood of a "dangling impurity" has also been explored [28]. Such a situation arises, for example, when a spin in one layer of a Heisenberg bilayer is removed, leaving an uncompensated spin 1/2. In this case, certain universal physics is predicted to occur, including power-law decays of the spin correlations. Accurate determinations of the associated exponents are available [28,29].

In this paper, we use exact diagonalization (ED) and the determinant quantum Monte Carlo (DQMC) methods to examine the physics of a single impurity in the PAM. Specifically, we compute the suppression of the singlet correlations about an impurity whose hybridization is in the AF regime, and which is embedded in a bulk singlet phase. By computing the AF correlations we can also infer the size of the AF region about the impurity. We examine the implications of these calculations on experiments on disordered heavy fermion materials.

II. MODEL AND METHODS

The uniform PAM describes a noninteracting conduction (d) band hybridized with localized (f) electrons,

$$
\mathcal{H} = -t \sum_{\langle ij \rangle, \sigma} (d^{\dagger}_{i\sigma} d_{j\sigma} + d^{\dagger}_{j\sigma} d_{i\sigma}) - V \sum_{i\sigma} (d^{\dagger}_{i\sigma} f_{i\sigma} + f^{\dagger}_{i\sigma} d_{i\sigma})
$$
$$
+ U_{\rm f} \sum_{i} \left(n^{\rm f}_{i\uparrow} - \frac{1}{2} \right) \left(n^{\rm f}_{i\downarrow} - \frac{1}{2} \right). \qquad (1)
$$

Here t is the hybridization between conduction orbitals with creation (destruction) operators $d^{\dagger}_{i\sigma}$ ($d_{i\sigma}$) on near neighbor sites $\langle ij \rangle$. $U_{\rm f}$ is the on-site interaction between spin-up and spin-down electrons in a collection of localized orbitals with creation (destruction) operators $f^{\dagger}_{i\sigma}$ ($f_{i\sigma}$) and number operators $n^{\rm f}_{i\sigma}$. V is the conduction-localized orbital hybridization. We have written the interaction term in H in "particle-hole" symmetric form, so that the lattice is half filled for all temperatures T and Hamiltonian parameters $t, U_{\rm f}, V$. Half filling optimizes the tendency for AF correlations, and also allows DQMC simulations at low temperature, since the sign problem is absent [30]. Our investigations here will be on a modification of Eq. (1) in which we introduce an "impurity" by changing the fd hybridization V to V_* on a single site j_0 of the lattice.

The magnetic physics of the PAM can be characterized by the spin-spin correlations, between two local (f) orbitals and

between a local and a conduction (d) orbital:

$$
\tilde{c}_{\rm ff}(j+r, j) = \langle (n^{\rm f}_{j+r\uparrow} - n^{\rm f}_{j+r\downarrow})(n^{\rm f}_{j\uparrow} - n^{\rm f}_{j\downarrow}) \rangle,
$$
$$
\tilde{c}_{\rm fd}(j+r, j) = \langle (n^{\rm f}_{j+r\uparrow} - n^{\rm f}_{j+r\downarrow})(n^{\rm d}_{j\uparrow} - n^{\rm d}_{j\downarrow}) \rangle. \qquad (2)
$$

These are translationally invariant, that is, functions only of separation r, for the uniform model and periodic boundary conditions. $\tilde{c}_{\rm ff}(j+r, j)$ characterizes the range of the intersite magnetic correlations between the local moments (mediated by the conduction electrons). One often focuses primarily on the local, $r = 0$ value $\tilde{c}_{\rm fd}(j, j)$ since it measures the on-site singlet correlations between the local and conduction electrons.

However, when an impurity is present at site j_0, translation invariance is broken. Since we are primarily interested in the alteration of magnetic order in the vicinity of the impurity, we will focus on the quantities

$$
c_{\rm ff}(r) = \tilde{c}_{\rm ff}(j_0 + r, j_0),
$$
$$
c_{\rm fd}(r) = \tilde{c}_{\rm fd}(j_0 + r, j_0 + r). \qquad (3)
$$

Note that the meaning of r is somewhat different for these two quantities. In the case of $c_{\rm ff}(r)$, the distance r represents how far a second f moment is from the f moment on the impurity site j_0 and thus has the "usual" meaning as a separation of two spin variables. $c_{\rm ff}(r)$ measures the range of AF correlations as one moves away from the impurity. In the case of $c_{\rm fd}(r)$, both spins are at a *common* distance r from the impurity—they sit on the same site—and r represents the distance of this pair of spins from the impurity. This is a useful definition, as we shall see, because it measures the "hole" which is created in a background of well-formed singlets which is created by a reduction of V at site j_0.

One way to quantify the effect of the impurity is through the changes in $c_{\rm ff}$ and $c_{\rm fd}$ due to its introduction. We define the impurity susceptibilities,

$$
\chi^{\rm imp}_{\rm ff}(r) = \frac{dc_{\rm ff}(r)}{dV} \bigg|_{V_* = V}, \qquad (4)
$$

to examine how the ff spin correlations between sites j_0 and $j_0 + r$ change due to a shift in impurity hybridization V_*.

The PAM can be solved exactly on small lattices using the Lanczos algorithm. Early work was on two and four site clusters in one dimension and found that small half-filled lattices are in a singlet phase for all $U_{\rm f}$ with, however, a near instability to AF [31]. This work was extended to larger lattices, in one dimension, by DQMC [32]. Here we will use ED to examine a single impurity in a one-dimensional PAM to gain initial insight into the effects on the AF and singlet correlations. The impurity will be characterized by a reduced value of the f-d hybridization V_*. A focus will be on examining how the bulk f-d hybridization affects the changes induced by the impurity. We will study geometries in which the impurity is placed at the end of the one-d chain. In both cases open boundary conditions are used.

ED, while providing useful initial insight, can examine only a small numbers of sites, hence the focus on the one-dimensional (1D) PAM. In fact, if one stays in one dimension, the density-matrix renormalization-group method is preferable, and has been used to study physics in the PAM [33,34]. Here we obtain results on larger lattices with

the determinant quantum Monte Carlo method [35], which we will use to study the PAM on a square lattice (i.e., in two dimensions). The DQMC approach introduces a space and imaginary time-dependent classical field to decouple the interaction U_f, allowing the fermion degrees of freedom to be integrated out analytically. The Boltzmann weight of the resulting classical Monte Carlo involves determinants of matrices (one for spin up and one for spin down) of dimension the number of sites in the lattice N. The computational cost scales as N^3, allowing for simulations on lattices at least an order of magnitude larger than for ED, where the cost scales exponentially with N. A limitation of DQMC is the "sign problem" which occurs when the fermion determinants become negative [30]. The sign problem does not occur in the Hamiltonian studied here, owing to its particle-hole symmetry (even in the presence of impurities), which guarantees that the spin-up and spin-down determinants have the same sign, so their product is always positive.

In this project, we have used "QUEST," a version of DQMC which allows the easy implementation of general geometries such as the impurity problem considered here. QUEST also contains a number of modifications to our "legacy" codes which improve speed and numerical stability. Some of its features are described in [36–40].

III. EXACT DIAGONALIZATION: 1D CHAIN

We begin our analysis of the effects of impurities in the PAM with exact diagonalization (Lanczos). While these are on small lattices, they have the advantage of easily accessing the ground state and large U_f, both of which are more challenging in DQMC. Because of the smallness of our cluster, $N = 6$ sites, we use open boundary conditions. The impurity is placed at one end of the chain.
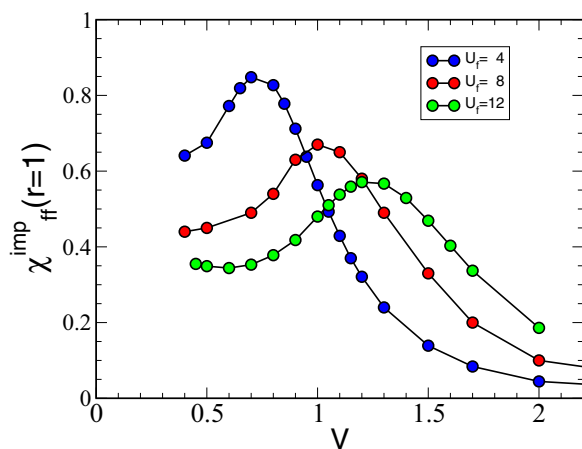

FIG. 1. Exact-diagonalization results for the f orbital impurity susceptibility on near-neighbor sites. $\chi_{\mathrm{ff}}^{\mathrm{imp}}(r = 1)$ probes the response of AF correlations to a local shift in $V \to V_* = V - dV$. $\chi_{\mathrm{ff}}^{\mathrm{imp}}(r = 1)$ is peaked at intermediate values of fd hybridization: At large V, deep in the singlet phase, $\chi_{\mathrm{ff}}^{\mathrm{imp}}(r = 1)$, is small. Similarly, $\chi_{\mathrm{ff}}^{\mathrm{imp}}(r = 1)$ also declines as $V \to 0$, deep in the AF regime. A maximum occurs at intermediate V. Results are given for on-site f electron repulsion $U_f = 4, 8, 12$.
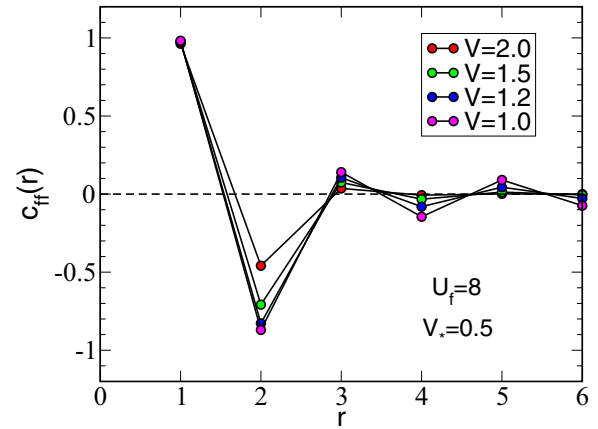

FIG. 2. ff spin-correlation function $c_{\mathrm{ff}}(r)$ for an impurity with $V_* = 0.5$ and different bulk V. As V approaches the singlet-AF crossover, spin correlations at long range develop. The f-orbital on-site repulsion $U_f = 8$.

We begin by considering the effect of a reduced hybridization V_* on the spin correlation between near-neighbor f orbitals. Figure 1 shows the impurity susceptibility on the localized orbitals, defined in Eq. (4). $\chi_{\mathrm{ff}}^{\mathrm{imp}}(r = 1)$ is peaked at intermediate values of the bulk V, i.e., between the AF and singlet phases. Although there is no AF-singlet transition in $d = 1$ [31], the maximum in $\chi_{\mathrm{ff}}^{\mathrm{imp}}(r = 1)$ is at crossover values corresponding to the $d = 2$ transition and also shifts to larger V as U_{ff} grows, as previously observed in DQMC calculations [23].

The AF correlations around an impurity site are shown in Figs. 2 and 3. Figure 2 contains the ff spin-correlation function $c_{\mathrm{ff}}(r)$ at fixed impurity hybridization $V_* = 0.5$ and varying bulk hybridization V. There is an almost perfectly formed local moment $c_{\mathrm{ff}}(r = 0) \approx 1$ and strong near-neighbor spin correlations $c_{\mathrm{ff}}(r = 1)$, which grow as V is reduced towards the location of the AF-singlet crossover. For $V = 2$, the AF
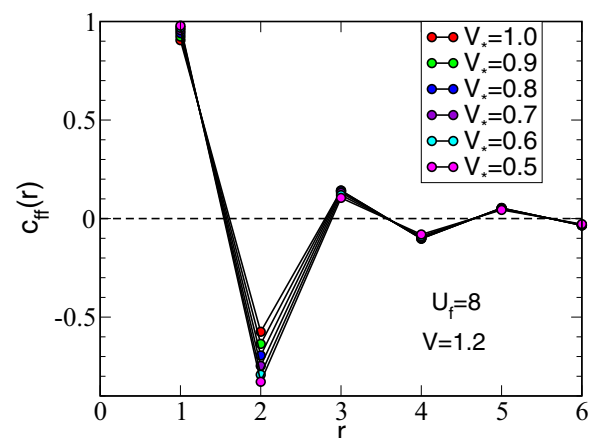

FIG. 3. Spin correlations in a system with bulk $V = 1.2$ for different impurity V_*. While there is some increase in the near-neighbor ff spin correlation function $c_{\mathrm{ff}}(r = 1)$, values at larger separation are quite insensitive to V_*. Here the f-orbital on-site repulsion $U_f = 8$.
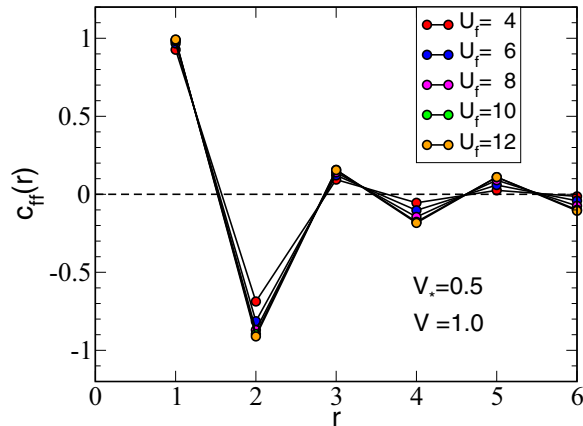
FIG. 4. The effect of U_f on spin correlations for fixed impurity and bulk hybridizations $V_* = 0.5$ and $V = 1.0$. The moment is nearly saturated even for $U_f = 4$, so that the main effect of increasing the on-site repulsion is a significant enhancement of the correlations at larger distances.

correlations are short-ranged, i.e., $c_{ff}(r > 1) \approx 0$. But an AF "droplet" develops around the impurity as V is decreased, so that by the time $V = 1.0$ there is a clearly discernible correlation even at $r = 6$, the maximal separation accessible on our cluster. Finally, Fig. 4 explores the effect of varying U_f for fixed impurity $V_* = 0.5$ and bulk $V = 1.0$. Larger on-site repulsion significantly increases $c_{ff}(r)$ at farther separations.

Figure 3 complements Fig. 2 by providing data for fixed V and varying V_*. While the near-neighbor correlation $c_{ff}(r = 1)$ shows some sensitivity to V_*, the longer range correlations $c_{ff}(r > 1)$ are unchanged as V_* varies. The conclusion is that the AF droplet is quite sensitive to the bulk hybridization, and develops to quite a large correlation length ξ near the AF-singlet crossover, but that the amount of reduction of the impurity hybridization V_* from the bulk value has little effect on ξ.

IV. RESULTS: QUANTUM MONTE CARLO

We now turn to results obtained with DQMC on $N = 8 \times 8$ lattices, much larger than the $N = 6$ cluster studied in exact diagonalization (ED). We used open boundary conditions on the small ED lattice, with the impurity at one end of the chain, to enable the study of effects of the impurity at distances r reasonably far away. The 8×8 lattice accessible in DQMC is large enough to allow data up to $r = 4\sqrt{2}$, even with the use of periodic boundary conditions (PBCs). This of course has the advantage of eliminating edge effects, so that the only breaking of translation invariance is due to the impurity. In the remainder of this section we first focus on the effect of the impurity on the spin-spin-correlation function, and then use these data to infer trends in the correlation length associated with the defect.

It is worth emphasizing that getting to large enough β (low T) poses some challenges for the DQMC simulation: The raw simulation time naively grows as β, but more realistically as β^p where $p \approx 2$ since there is an increase in statistical noise (requiring longer runs to get the same error bar) and also an accumulation of round off errors which necessitates more frequent reorthogonalization of the matrix products.
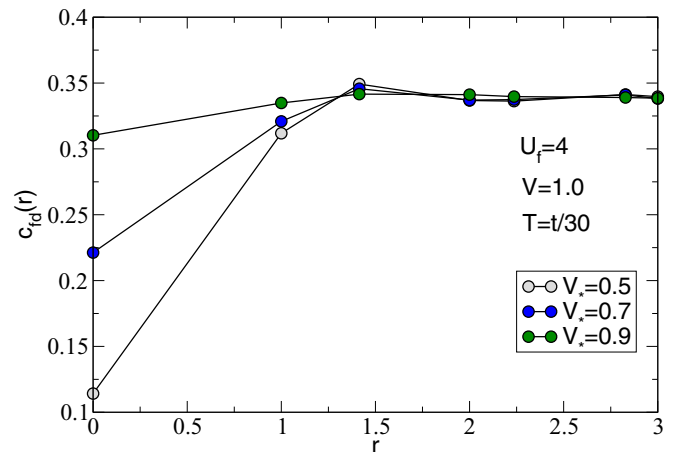

FIG. 5. The fd singlet correlator $c_{fd}(r)$ as a function of distance r from the impurity is shown for bulk hybridization $V = 1$ and different impurity hybridizations V_*. Moving the impurity deeper into the AF phase steadily reduces the singlet directly on the defect site ($r = 0$). However, the spatial extent of this hole does not increase as V_* decreases. Here the bulk hybridization $V = 1.0$. The temperature $T = t/30$. The f-orbital on-site repulsion $U_f = 4$.

A. Spatial variation of singlet correlations in the vicinity of the impurity

One way to characterize the effect of a magnetic impurity is to consider the size and range of the "hole" it digs in the bulk singlet correlations. In Fig. 5 the effect of changing the strength of the impurity $V_* = 0.1, 0.3, 0.5$ on the local singlet correlator $c_{fd}(r)$ at distance r from the defect is examined. Here we choose $V = 1.0$ which is near the bulk AF-singlet boundary [23]. There is a systematic reduction in the singlet $c_{fd}(r = 0)$ directly on the defect as its coupling V_* moves deeper into the AF regime. The range of the reduction of singlets on $r \neq 0$ sites in its vicinity is basically independent of V_*. Indeed,
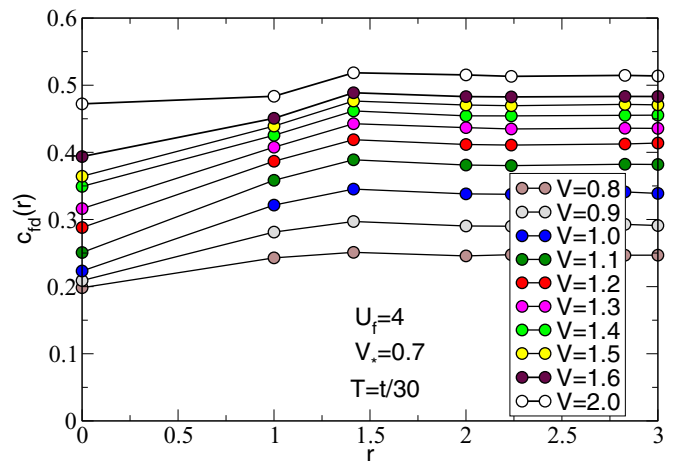

FIG. 6. Spin correlations between local and conduction electrons, $c_{fd}(r)$, are shown for different bulk V and fixed impurity $V_* = 0.7$. All curves exhibit a similar short-range reduction of singlet correlations near the impurity, however, this reduction is largest for intermediate V. (See also Fig. 6.) The temperature $T = t/30$. The f-orbital on-site repulsion $U_f = 4$.
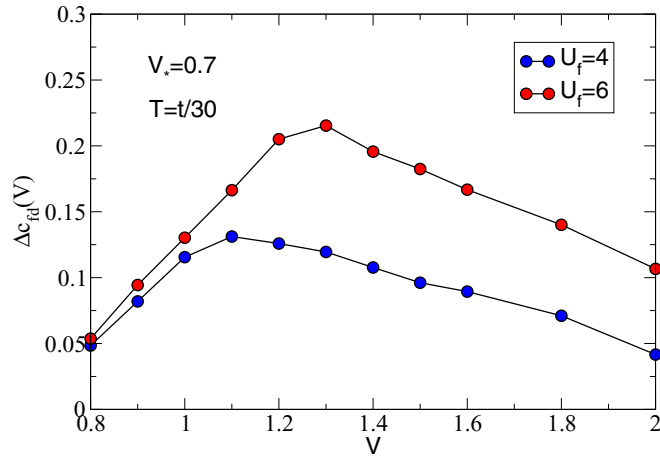
FIG. 7. The reduction of the local-conduction spin correlator, $c_{fd}(r = 0)$, from the asymptotic value $c_{fd}(r \to \infty)$ shown for different bulk hybridization V. The temperature $T = t/30$. Results are shown for on-site f electron repulsion $U_f = 4, 6$. Here, for $U_f = 4$, the hole gets deeper as V is reduced from $V = 2.0$ and becomes deepest for $V = 1.1$, after which it is again reduced. This tendency fits well with the picture that the effect of an impurity is largest near the AF-singlet QCP, e.g., as we show in Fig. 1.

$c_{fd}(r)$ does not differ appreciably from the bulk $V_* = V$ values beyond on-site ($r = 0$) and near-neighbor ($r = 1$) separations.

Figure 6 complements Fig. 5 by presenting the local-conduction spin correlations, $c_{fd}(r)$, for fixed impurity $V_* = 0.7$ and different bulk V. There is a uniform upward shift for all r in the curves with larger V, reflecting the greater tendency for singlet formation throughout the lattice. The suppression of the singlet correlations at the position of the defect $r = 0$ confirm the nonmonotonic trend of Fig. 1.

This is more cleanly presented in Fig. 7. We calculate the reduction of fd correlations in the vicinity of the defect,

$$\Delta c_{fd} = c_{fd}(r \to \infty) - c_{fd}(r = 0). \quad (5)$$

Figure 7 shows the bulk hybridization dependence of $\Delta c_{fd}(V)$. The largest reduction occurs at intermediate V, i.e., in the vicinity of the AF-singlet quantum phase transition, in accordance with the ED results shown in Fig. 1. We also calculate $\Delta c_{fd}(V)$ at higher f-orbital on-site repulsion $U_f = 6$. The occurrence of an "optimal V_*" is even more evident, and, to the extent that the position of this maximum acts as a proxy for the location V_c of the AF-singlet transition in the uniform periodic Anderson model, indicates that V_c is an increasing function of U_f. This is consistent with the phase diagram of [23].

Because V_* is fixed in Figs. 6 and 7, as V increases the "defect strength" $V - V_*$ is also increasing. It is also interesting to ask what happens as a function of bulk V if $V - V_*$ is held fixed, Fig. 8. Here one sees a monotonic behavior of $\Delta c_{fd}(V)$.

B. Spatial variation of AF correlations in the vicinity of the impurity

After characterizing the effect of the AF impurity in terms of its effect on the on-site singlet correlation, we turn now to
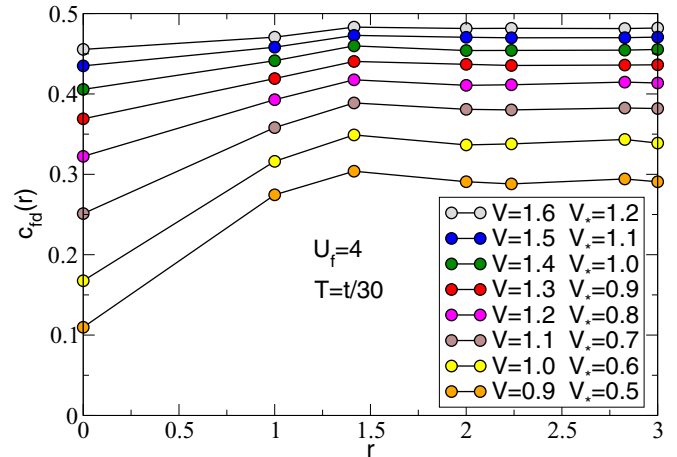

FIG. 8. On-site singlet correlator $c_{fd}(r)$ as a function of distance r from the defect. Here the bulk hybridization V is varied at *fixed $V - V_* = 0.4$*. The maximum in the reduction $\Delta c_{fd}(V)$ at intermediate V is absent. The temperature $T = t/30$ and the f-orbital on-site repulsion $U_f = 4$.

a determination of the size and strength of the AF "droplet" it induces.

We begin, in Fig. 9, by showing the spin-spin correlator $c_{ff}(r)$ between the f moment on the defect site ($V_* = 0.7$) and an f moment at separation r [see Eq. (3)]. When the bulk $V = 0.8, 0.9, 1.0, 1.1$ is also in the AF regime, these spin correlations are long ranged: Long-range AF correlations can only survive when the bulk V is in the AF phase. Otherwise the impurity can only create a local AF cloud. Figure 10 focuses on these effects in the vicinity of the AF-singlet transition. The bulk $V = 1.2$ is fixed and different impurity V_* are considered. The AF correlations are largely independent of V_*. However, in Fig. 9, as one crosses over into the bulk singlet, $V = 1.2, 1.6, 2.0$ the range of the AF droplet is finite. The
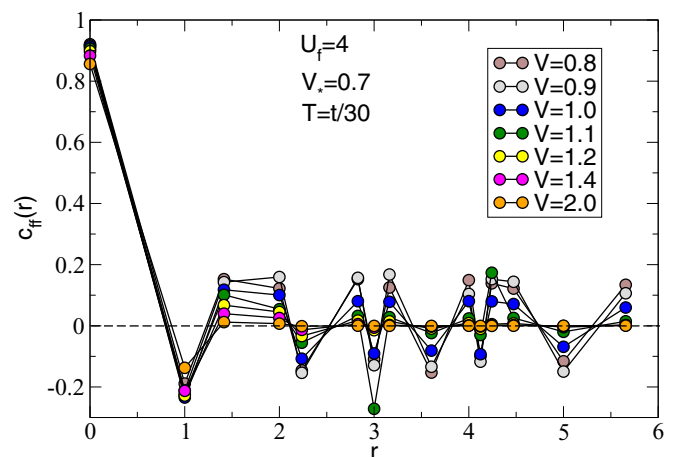

FIG. 9. Spin-correlation function $c_{ff}(r)$ between two local (f) orbitals. A defect with impurity hybridization $V_* = 0.7$ is present in different background materials with varying V. There are long-range correlations for V in the AF regime, but the impurity can only induce AF order locally if V is large. The temperature $T = t/30$ and the f-orbital on-site repulsion $U_f = 4$.
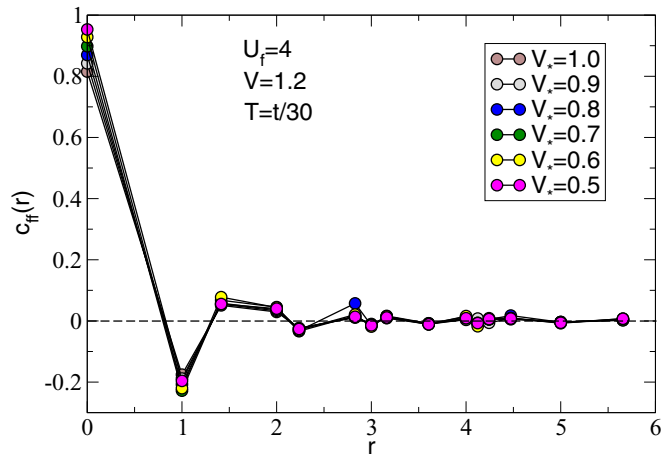
FIG. 10. ff electron spin-correlation function $c_{\text{ff}}(r)$ for bulk hybridization $V = 1.2$ and different impurity hybridizations V_*. As V_* decreases the short-range AF order with near neighbor $(1,0)$ becomes deeper. The temperature $T = t/30$. The f-orbital on-site repulsion $U_{\text{f}} = 4$.

suppression of $c_{\text{ff}}(r)$ at low V is a finite temperature effect: The strength of the RKKY coupling goes as V^2, so as V decreases one needs to go to lower temperatures to access the ground state. Our results here are at fixed $\beta = 30$. If we were to lower T further (increase β) at $V = 0.5$ the AF correlations would substantially increase.

C. AF cloud size and correlation length

As discussed in the Introduction, a key experimental quantity of interest is the size of the AF island, e.g., that created by a Cd impurity in CeCoIn$_5$. The preceding figures, which show $c_{\text{ff}}(r)$, provide a qualitative picture, which here we will quantify somewhat more precisely. To begin, it is useful to focus more closely on the short-range spin correlations. Figure 11 shows the dependence on V of $c_{\text{ff}}(r)$, for first $r = (1,0)$, second $r = (1,1)$, and third $r = (2,0)$ neighbors.
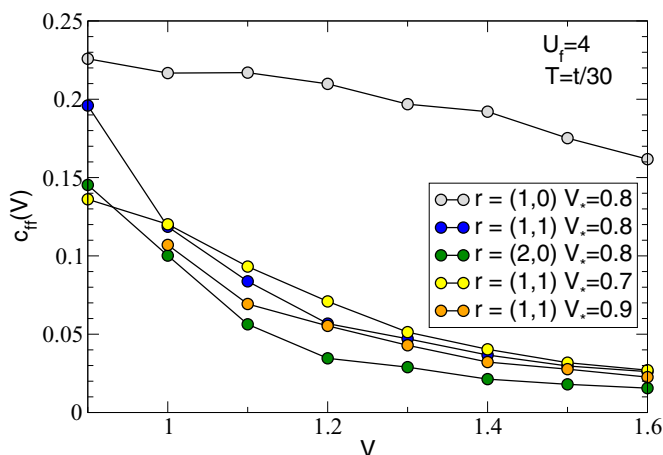

FIG. 11. Spin correlations between local electrons, $c_{\text{ff}}(r)$, for near neighbors $(1,0)$, $(1,1)$, and $(2,0)$. $c_{\text{ff}}(r)$ grows as V approaches the AF-singlet crossover. The temperature $T = t/30$. The f-orbital on-site repulsion $U_{\text{f}} = 4$.
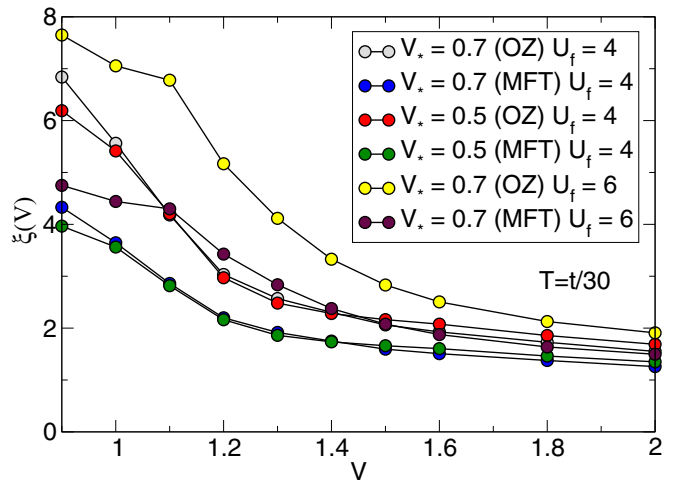

FIG. 12. Correlation length vs V given for fixed impurity $V_* = 0.5, 0.7$. Results are shown for two values of the on-site f electron repulsion $U_{\text{f}} = 4, 6$. OZ (MFT) refer to fits to an Ornstein-Zernike (mean-field theory) form. Although the values of ξ are sensitive to this choice, the main qualitative feature of the curves is not. It shows an evolution from a flat $\xi \approx 2$ at large V to a rising $\xi \approx 4$–6 (at $U_{\text{f}} = 4$), indicating larger AF regions. The temperature $T = t/30$.

$c_{\text{ff}}(r = 1,0)$ is substantial through the AF-singlet transition region, showing no signature at V_c. This "blindness" to transitions is of course characteristic of short-range correlations. E.g., in the Ising model the first neighbor spin correlation is just the energy, which is smooth through T_c. $c_{\text{ff}}(r = 1,1)$ and $c_{\text{ff}}(r = 0,2)$ fall more rapidly through V_c. Ultimately, of course, at large distances $c_{\text{ff}}(|\vec{r}| \to \infty)$ is proportional to the square of the AF order parameter and would vanish for $V > V_c$. At $r = (1,1)$, data for several values $V_* = 0.7, 0.8, 0.9$ are given. $c_{\text{ff}}(r = 1,1)$ is not very sensitive to the precise value of V_*, especially for V large, where all three curves coincide (see Fig. 11).

The plots of $c_{\text{ff}}(r)$ already give a qualitative indication of the value of the correlation length ξ. We can make this somewhat more quantitative by fitting the magnitude of $c_{\text{ff}}(r)$ either to a mean-field or Ornstein-Zernike form to obtain the AF correlation length ξ. This is not expected to be too precise since these functional forms describe the asymptotic behavior at large distances which are not sampled on our finite lattices. Nevertheless, Fig. 12 shows the results of our DQMC simulations for the dependence of ξ on bulk hybrdization V for fixed impurity $V_* = 0.5, 0.7$ and two values of U_{f}. The conclusion is that the size of the AF cloud is fairly small, $\xi \lesssim 2$, unless the bulk V is close to, or below, the AF-singlet QCP. It takes a value $\xi \sim 3$ right at $V = V_c \sim 1.1$ [23]. Well into the AF phase, ξ is of the order of the linear size of the lattice, indicating that there is long-range order throughout the 8×8 cluster studied here. In this case, ξ is expected to scale with the linear size, whereas if ξ is only a few lattice spacings it has likely converged on 8×8 clusters. Finite-size scaling can be used to establish order in the thermodynamic limit [23,41]. The change in slope from the flat region $\xi \approx 2$ to a rising ξ occurs as one approaches the bulk critical point $V_c \approx 1.1$. Indeed, although it is not so easy to tell from the scatter in the data, there is some indication of an inflection point (maximal
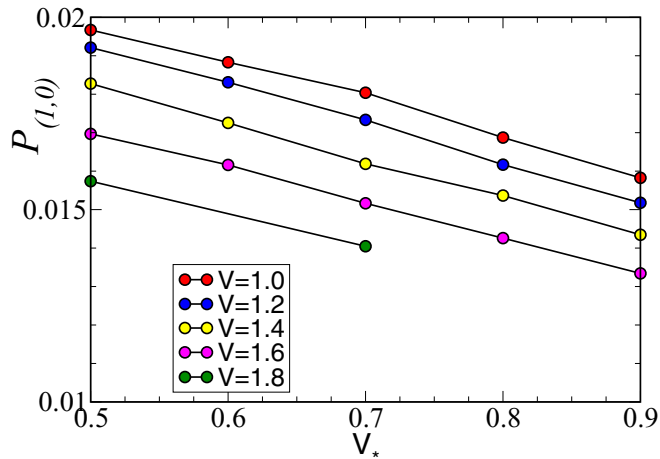
FIG. 13. Near-neighbor d-wave pair correlations as a function of impurity hybridization V_* for different bulk hybridizations for $\beta t = 30$ and $U_f = 4$.

slope of growth of ξ) at the QCP. It has been noted in quantum spin models [27,29] that the effect of impurities is localized in the spin gap (singlet) phase, but that at the QCP critical spin correlations instead exhibit power-law decays in space and imaginary time.

D. Pairing correlations

The previous sections have focused on the effects of spatial inhomogeneities on magnetic correlations, a problem which has also been explored at surfaces where the reduced coordination number can decrease the bandwidth and hence, somewhat counterintuitively, enhance magnetism despite the lower number of neighbors [42,43].

Recent work on superconductivity in the PAM has explored the effect of frustration in the doped system [44], as well as the evolution of the symmetry of the order parameter with interaction strength in its strong-coupling limit, the Kondo lattice model [45]. Here we describe the effect of the impurity on d-wave pairing correlations about the impurity site j_0,

$$\mathcal{P}_r = \langle \Delta_{j_0+r} \Delta_{j_0}^\dagger \rangle,$$
$$\Delta_{j_0}^\dagger = \left(c_{j_0+x,\downarrow}^\dagger - c_{j_0+y,\downarrow}^\dagger + c_{j_0-x,\downarrow}^\dagger - c_{j_0-y,\downarrow}^\dagger \right) c_{j_0,\uparrow}^\dagger. \quad (6)$$

Figure 13 shows the evolution of $\mathcal{P}_{(1,0)}$ with V_* for different bulk hybridizations. $\mathcal{P}_{(1,0)}$ steadily increases as the impurity site hybridization is reduced, that is, as the degree of inhomogeneity grows. The enhancement of pairing correlations around impurities appears to be a not uncommon feature of tight-binding models in which magnetic correlations are a primary instability. The effect appears prominently, for example, in striped [46] and plaquette [47] Hubbard Hamiltonians, with a key issue being an intermediate degree of anisotropy which optimizes superconducting correlations [48].

V. CONCLUSIONS

Much of our understanding, through QMC, of the effects of randomness in quantum antiferromagnets and their

implications for materials like disordered heavy fermion compounds has been developed with spin models like the transverse field Ising or Heisenberg bilayer Hamiltonians [17,18,24–26,49,50]. In this paper, we have examined the physics of a single impurity on the competition between antiferromagnetic and singlet correlations in the periodic Anderson model, i.e., in the more computationally challenging case of an *itinerant* electron model. An impurity with a d-f hybridization in the AF regime suppresses singlet correlations in its vicinity, and at the same time induces an AF domain. As the f-d hybridization of the bulk approaches the AF transition from the singlet side, the impurity becomes increasingly effective at inducing AF correlations.

Our work parallels earlier Hartree-Fock studies of disorder in cuprate superconductors, modeled with the single band Hubbard Hamiltonian [9]. There, the level of doping x and the on-site Hubbard interaction U are used to tune the system in the neighborhood of magnetic and superconducting phase transitions, and the effect of impurities is then explored. Analogously, we have here examined an impurity in a multiband periodic Anderson model which has a singlet-AF quantum phase transition.

These results provide an important confirmation for the experimental observation of AF droplets in quantum critical CeCoIn$_5$. In this material, the AF droplets were observed to disappear under pressure. Increasing pressure corresponds to increasing V as the d and f orbital overlap increases. As our simulations indicate, the size and extent of the AF droplets decrease with increasing V as the system is tuned away from the QCP. These studies also suggest that heavy fermion systems that can be tuned to a QCP under pressure, such as CeRhIn$_5$, may also exhibit similar behavior [51,52]. An important question is whether "chemical pressure" in which dopants are added to either expand or contract the lattice actually affects the electronic degrees of freedom by modifying the local hybridization. In the case of Cd-doped CeCoIn$_5$, the Cd has no $5p$ electrons to hybridize with the neighboring Ce, thus our introduction of $V_* < V$ is a reasonable approach. Sn doping, on the other hand, with one extra $5p$ electron, does not exhibit AF order [53].

The ED method for the PAM is limited to systems of around ten sites. DQMC calculations can be performed on several hundred sites. Even so, in two dimensions, the lattices accessible to DQMC are only 10–20 sites in linear extent. Thus it is difficult to perform definitive studies of multiple impurities and their surrounding domains. This is a crucial question, because the overlapping of AF domains about individual impurities, and the lack of frustration in such overlap, is believed to lead to AF long-range order [54]. Quantum spin models like the Heisenberg bilayer can, however, be explored on much larger lattices. Future work will focus on examining randomness and the AF-singlet transition for such quantum spin models.

[1] P. A. Lee and T. V. Ramakrishnan, Disordered electronic systems, Rev. Mod. Phys. **57**, 287 (1985).

[2] D. Belitz and T. R. Kirkpatrick, The anderson-mott transition, Rev. Mod. Phys. **66**, 261 (1994).

[3] M. Ulmke, V. Janiš, and D. Vollhardt, Anderson-hubbard model in infinite dimensions, Phys. Rev. B **51**, 10411 (1995).

[4] M. Ulmke and R. Scalettar, Magnetic correlations in the two dimensional anderson-hubbard model, Phys. Rev. B **55**, 4149 (1997).

[5] S. V. Kravchenko and M. P. Sarachik, Metal-insulator transition in two dimensional electron systems, Rep. Prog. Phys. **67**, 1 (2004).

[6] E. Miranda and V. Dobrosavljevic, Disorder-driven non-fermi liquid behavior of correlated electrons, Rep. Prog. Phys. **68**, 2337 (2005).

[7] A. M. Goldman, Superconductor-insulator transitions, Int. J. Mod. Phys. B **24**, 4081 (2010).

[8] H. Kimura, M. Kofu, Y. Matsumoto, and K. Hirota, Novel In-Gap Spin State in Zn-Doped $La_{1.85}Sr_{0.15}CuO_4$, Phys. Rev. Lett. **91**, 067002 (2003).

[9] B. M. Andersen, P. J. Hirschfeld, A. P. Kampf, and M. Schmid, Disorder-Induced Static Antiferromagnetism in Cuprate Superconductors, Phys. Rev. Lett. **99**, 147002 (2007).

[10] A. J. Millis, D. K. Morr, and J. Schmalian, Local Defect in Metallic Quantum Critical Systems, Phys. Rev. Lett. **87**, 167202 (2001).

[11] J. C. Phillips, A. Saxena, and A. R. Bishop, Pseudogaps, dopants, and strong disorder in cuprate high-temperature superconductors, Rep. Prog. Phys. **66**, 2111 (2003).

[12] B. Keimer, S. A. Kivelson, M. R. Norman, S. Uchida, and J. Zaanen, From quantum matter to high-temperature superconductivity in copper oxides, Nature (London) **518**, 179 (2015).

[13] S. Seo, X. Lu, J.-X. Zhu, R. R. Urbano, N. Curro, E. D. Bauer, V. A. Sidorov, L. D. Pham, T. Park, Z. Fisk, and J. D. Thompson, Disorder in quantum critical superconductors, Nat. Phys. **10**, 120 (2014).

[14] R. R. Urbano, B.-L. Young, N. J. Curro, J. D. Thompson, L. D. Pham, and Z. Fisk, Interacting Antiferromagnetic Droplets in Quantum Critical $CeCoIn_5$, Phys. Rev. Lett. **99**, 146402 (2007).

[15] O. Stockert, H. v. Löhneysen, A. Rosch, N. Pyka, and M. Loewenhaupt, Two-Dimensional Fluctuations at the Quantum-Critical Point of $CeCu_{6-x}Au_x$, Phys. Rev. Lett. **80**, 5627 (1998).

[16] S. Friedemann, T. Westerkamp, M. Brando, N. Oeschler, S. Wirth, P. Gegenwart, C. Krellner, C. Geibel, and F. Steglich, Detaching the antiferromagnetic quantum critical point from the fermi-surface reconstruction in $YbRh_2Si_2$, Nat. Phys. **5**, 465 (2009).

[17] A. H. Castro Neto, G. Castilla, and B. A. Jones, Non-Fermi Liquid Behavior and Griffiths Phase in f-Electron Compounds, Phys. Rev. Lett. **81**, 3531 (1998).

[18] T. Vojta, Quantum griffiths effects and smeared phase transitions in metals: Theory and experiment, J. Low Temp. Phys. **161**, 299 (2010).

[19] P. W. Anderson, Localized magnetic states in metals, Phys. Rev. **124**, 41 (1961).

[20] M. A. Ruderman and C. Kittel, Indirect exchange coupling of nuclear magnetic moments, Phys. Rev. **96**, 99 (1954).

[21] T. Kasuya, A theory of metallic ferro- and antiferromagnetism on zener's model, Prog. Theor. Phys. **16**, 45 (1956).

[22] K. Yosida, Magnetic properties of Cu-Mn alloys, Phys. Rev. **106**, 893 (1957).

[23] M. Vekić, J. W. Cannon, D. J. Scalapino, R. T. Scalettar, and R. L. Sugar, Competition between Antiferromagnetic Order and Spin-Liquid Behavior in the Two-Dimensional Periodic Anderson Model at Half Filling, Phys. Rev. Lett. **74**, 2367 (1995).

[24] A. W. Sandvik and D. J. Scalapino, Order-Disorder Transition in a Two-Layer Quantum Antiferromagnet, Phys. Rev. Lett. **72**, 2777 (1994).

[25] L. Wang, K. S. D. Beach, and A. W. Sandvik, High-precision finite-size scaling analysis of the quantum-critical point of $s = 1/2$ heisenberg antiferromagnetic bilayers, Phys. Rev. B **73**, 014431 (2006).

[26] A. W. Sandvik, Quantum Criticality and Percolation in Dimer-Diluted Two-Dimensional Antiferromagnets, Phys. Rev. Lett. **96**, 207201 (2006).

[27] K. H. Höglund and A. W. Sandvik, Impurity effects at finite temperature in the two-dimensional s=1/2 heisenberg antiferromagnet, Phys. Rev. B **70**, 024406 (2004).

[28] K. H. Höglund, A. W. Sandvik, and S. Sachdev, Impurity Induced Spin Texture in Quantum Critical 2D Antiferromagnets, Phys. Rev. Lett. **98**, 087203 (2007).

[29] S. Sachdev, C. Buragohain, and M. Vojta, Quantum impurity in a nearly-critical two dimensional antiferromagnet, Science **286**, 2479 (1999).

[30] E. Y. Loh, J. E. Gubernatis, R. T. Scalettar, S. R. White, D. J. Scalapino, and R. L. Sugar, Sign problem in the numerical simulation of many-electron systems, Phys. Rev. B **41**, 9301 (1990).

[31] R. Jullien and R. M. Martin, Ground-state and low-lying excitations of the periodic anderson hamiltonian in one dimension from finite-cell calculations, Phys. Rev. B **26**, 6173 (1982).

[32] R. Blankenbecler, J. R. Fulco, W. Gill, and D. J. Scalapino, Ground-State Properties of the Periodic Anderson Model, Phys. Rev. Lett. **58**, 411 (1987).

[33] M. Guerrero and C. C. Yu, Kondo insulators modeled by the one-dimensional anderson lattice: A numerical-renormalization-group study, Phys. Rev. B **51**, 10301 (1995).

[34] N. Shibata and K. Ueda, The one-dimensional kondo lattice model studied by the density matrix renormalization group method, J. Phys: Condens. Matter **11**, 4289 (1999).

[35] R. Blankenbecler, D. J. Scalapino, and R. L. Sugar, Monte Carlo calculations of coupled boson-fermion systems. I, Phys. Rev. D **24**, 2278 (1981).

[36] Z. Bai, W. Chen, R. Scalettar, and I. Yamazaki, Numerical methods for quantum monte carlo simulations of the hubbard model, in *Multi-Scale Phenomena in Complex Fluids*, edited by T. Y. Hou, C. Liu, and J.-G. Liu, Contemporaary Applied Mathematics (Higher Education Press and World Scientific, Beijing, 2009), Vol. 12, p. 1–100.

[37] C. R. Lee, I. H. Chung, and Z. Bai, Parallelization of DQMC simulation for strongly correlated electron systems, in *IEEE International Symposium on Parallel & Distributed Processing (IPDPS)* (IEEE, New York, 2010), p. 1.

[38] A. Tomas, C. C. Chang, R. Scalettar, and Z. Bai, in *IEEE International Symposium on Parallel & Distributed Processing (IPDPS)* (IEEE, New York, 2012), p. 308.

[39] S. Gogolenko, Z. Bai, and R. Scalettar, Structured orthogonal inversion of block p-cyclic matrices on multicores with GPU accelerators, in *Euro-Par 2014 Parallel Processing, Switzerland* (Springer, New York, 2014), p. 524.

[40] C. C. Chang, S. Gogolenko, J. Perez, Z. Bai, and R. T. Scalettar, Recent advances in determinant quantum Monte Carlo, Philos. Mag. **95**, 1260 (2015).

[41] C. N. Varney, C. R. Lee, Z. J. Bai, S. Chiesa, M. Jarrell, and R. T. Scalettar, Quantum Monte Carlo study of the two-dimensional fermion Hubbard model, Phys. Rev. B **80**, 075116 (2009).

[42] A. K. Kazanskii, A. S. Kondratrev, and V. M. Uzdin, Description of magnetically ordered stratified state in the periodic Anderson model, JETP **67**, 372 (1988).

[43] F. Zhang, S. Thevuthasan, R. T. Scalettar, R. R. P. Singh, and C. S. Fadley, A Monte Carlo study of magnetic order at ferromagnetic and antiferromagnetic surfaces: Implications for spin-polarized photoelectric diffraction, Phys. Rev. B **51**, 12468 (1995).

[44] W. Wu and A. M. S. Tremblay, d-Wave Superconductivity in the Frustrated Two-Dimensional Periodic Anderson Model, Phys. Rev. X **5**, 011019 (2015).

[45] J. Otsuki, Competing d-Wave and p-Wave Spin-Singlet Superconductivities in the Two-Dimensional Kondo Lattice, Phys. Rev. Lett. **115**, 036404 (2015).

[46] E. Arrigoni, E. Fradkin, and S. A. Kivelson, Mechanism of high-temperature superconductivity in a striped hubbard model, Phys. Rev. B **69**, 214519 (2004).

[47] W. F. Tsai, H. Yao, and S. A. Kivelson, Myriad phases of the checkerboard Hubbard model, Phys. Rev. B **76**, 161104(R) (2007).

[48] T. Ying, R. Mondaini, X. D. Sun, T. Paiva, R. M. Fye, and R. T. Scalettar, Determinant quantum Monte Carlo study of d-wave pairing in the plaquette Hubbard Hamiltonian, Phys. Rev. B **90**, 075121 (2014).

[49] M. Guo, R. N. Bhatt, and D. A. Huse, Quantum griffiths singularities in the transverse-field Ising spin glass, Phys. Rev. B **54**, 3336 (1996).

[50] A. P. Young, Finite-temperature and dynamical properties of the random transverse-field Ising spin chain, Phys. Rev. B **56**, 11691 (1997).

[51] H. Hegger, C. Petrovic, E. G. Moshopoulou, M. F. Hundley, J. L. Sarrao, Z. Fisk, and J. D. Thompson, Pressure-Induced Superconductivity in Quasi-2D CeRhIn$_5$, Phys. Rev. Lett. **84**, 4986 (2000).

[52] T. Park, V. A. Sidorov, H. Lee, F. Ronning, E. D. Bauer, J. L. Sarrao, and J. D. Thompson, Unconventional quantum criticality in the pressure-induced heavy-fermion superconductor CeRhIn$_5$, J. Phys.: Condens. Matter **23**, 094218 (2011).

[53] E. D. Bauer, C. Capan, F. Ronning, R. Movshovich, J. D. Thompson, and J. L. Sarrao, Superconductivity in CeCoIn$_{5-x}$Sn$_x$: Veil Over an Ordered State or Novel Quantum Critical Point? Phys. Rev. Lett. **94**, 047001 (2005).

[54] D. Kivelson, S. A. Kivelson, X. L. Zhao, Z. Nussinov, and G. Tarjus, A thermodynamic theory of supercooled liquids, Physica A **219**, 27 (1995).